

Electro-optically spectrum narrowed, multiline intracavity optical parametric oscillators

W. K. CHANG,^{1,2} H. P. CHUNG,¹ Y. Y. CHOU,¹ R. GEISS,³ S. D. YANG,⁴ T. PERTSCH,³ AND Y. H. CHEN^{1,*}

¹Department of Optics and Photonics, National Central University, Zhongli 320, Taiwan

²Brain Research Center, National Tsinghua University, Hsinchu 30013, Taiwan

³Institute of Applied Physics, Abbe Center of Photonics, Friedrich-Schiller-Universität Jena, Max-Wien-Platz 1, 07743 Jena, Germany

⁴Institute of Photonics Technologies, Department of Electrical Engineering, National Tsinghua University, Hsinchu 30013, Taiwan

*yhchen@dop.ncu.edu.tw

Abstract: We report on the first building of an active spectral narrowing mechanism in a pulsed, multiline optical parametric oscillator (OPO) based on a novel aperiodically poled lithium niobate (APPLN) device constructed using the aperiodic optical superlattice technique. The APPLN device functions simultaneously in the system as a multi-channel optical parametric down converter (OPDC) and an electro-optic (EO) gain spectral filter working on the corresponding (multiple) signal bands. When the APPLN OPO was installed in a diode pumped Nd:YVO₄ laser system, highly narrowed dual-wavelength signal lines (at 1540 and 1550 nm) were observed at the output of the system through EO control of the APPLN. Correspondingly, an enhancement of the power spectral density of the source by a factor of ~7.8 with respect to the system operated in passive mode was found.

© 2016 Optical Society of America

OCIS codes: (230.2090) Electro-optical devices; (190.4970) Parametric oscillators and amplifiers.

References and links

1. M. Wirth, A. Fix, P. Mahnke, H. Schwarzer, F. Schrandt, and G. Ehret, "The airborne multi-wavelength water vapor differential absorption lidar WALES: system design and performance," *Appl. Phys. B* **96**(1), 201–213 (2009).
2. M. H. Chou, J. Hauden, M. A. Arbore, and M. M. Fejer, "1.5- μ m-band wavelength conversion based on difference-frequency generation in LiNbO₃ waveguides with integrated coupling structures," *Opt. Lett.* **23**(13), 1004–1006 (1998).
3. K. Kawase, T. Hatanaka, H. Takahashi, K. Nakamura, T. Taniuchi, and H. Ito, "Tunable terahertz-wave generation from DAST crystal by dual signal-wave parametric oscillation of periodically poled lithium niobate," *Opt. Lett.* **25**(23), 1714–1716 (2000).
4. C. L. Wang and C. L. Pan, "Tunable dual-wavelength operation of a diode array with an external grating-loaded cavity," *Appl. Phys. Lett.* **64**(23), 3089–3091 (1994).
5. X. Z. Wang, Z. F. Wang, Y. K. Bu, L. J. Chen, G. X. Cai, and Z. P. Cai, "A 1064- and 1074-nm dual-wavelength Nd:YAG laser using a Fabry–Perot band-pass filter as output mirror," *IEEE Photonics J.* **6**(4), 1 (2014).
6. T. M. J. Kendall, W. A. Clarkson, P. J. Hardmar, G. W. Ross, and D. C. Hanna, "Multiline optical parametric oscillators based on periodically poled lithium niobate," in *Conference on Lasers and Electro-Optics*, OSA Technical Digest (Optical Society of America, 2000), paper CMC2.
7. Y. H. Chen, W. K. Chang, H. P. Chung, B. Z. Liu, C. H. Tseng, and J. W. Chang, "Tunable, pulsed multiline intracavity optical parametric oscillator using two-dimensional MgO: periodically poled lithium niobate-aperiodically poled lithium niobate," *Opt. Lett.* **38**(18), 3507–3509 (2013).
8. J. Y. Lai, Y. J. Liu, H. Y. Wu, Y. H. Chen, and S. D. Yang, "Engineered multiwavelength conversion using nonperiodic optical superlattice optimized by genetic algorithm," *Opt. Express* **18**(5), 5328–5337 (2010).
9. C. L. Chang, Y. H. Chen, C. H. Lin, and J. Y. Chang, "Monolithically integrated multi-wavelength filter and second harmonic generator in aperiodically poled lithium niobate," *Opt. Express* **16**(22), 18535–18544 (2008).
10. S. J. Brosnan and R. L. Byer, "Optical parametric oscillator threshold and linewidth studies," *IEEE J. Quantum Electron.* **15**(6), 415–431 (1979).
11. L. A. W. Gloster, I. T. McKinnie, Z. X. Jiang, T. A. King, J. M. Boon-Engering, W. E. van der Veer, and W. Hogervorst, "Narrow-band β -BaB₂O₄ optical parametric oscillator in a grazing-incidence configuration," *J. Opt. Soc. Am. B* **12**(11), 2117–2121 (1995).

12. B. Jacobsson, M. Tiihonen, V. Pasiskevicius, and F. Laurell, "Narrowband bulk Bragg grating optical parametric oscillator," *Opt. Lett.* **30**(17), 2281–2283 (2005).
13. C. H. Lin, Y. H. Chen, S. W. Lin, C. L. Chang, Y. C. Huang, and J. Y. Chang, "Electro-optic narrowband multi-wavelength filter in aperiodically poled lithium niobate," *Opt. Express* **15**(15), 9859–9866 (2007).
14. J. W. Chang, H. F. Yau, H. P. Chung, W. K. Chang, and Y. H. Chen, "Characterization and analysis of finite-beam Bragg diffraction in a periodically poled lithium niobate electro-optic grating," *Appl. Opt.* **53**(24), 5312–5321 (2014).
15. Y. H. Chen, J. W. Chang, C. H. Lin, W. K. Chang, N. Hsu, Y. Y. Lai, Q. H. Tseng, R. Geiss, T. Pertsch, and S. S. Yang, "Spectral narrowing and manipulation in an optical parametric oscillator using periodically poled lithium niobate electro-optic polarization-mode converters," *Opt. Lett.* **36**(12), 2345–2347 (2011).
16. H. P. Chung, W. K. Chang, C. H. Tseng, R. Geiss, T. Pertsch, and Y. H. Chen, "Electro-Optically Spectrum Tailorable Intracavity Optical Parametric Oscillator," *Opt. Lett.* **40**(22), 5132–5135 (2015).
17. B. Y. Gu, B. Z. Dong, Y. Zhang, and G. Z. Yang, "Enhanced harmonic generation in aperiodic optical superlattices," *Appl. Phys. Lett.* **75**(15), 2175–2177 (1999).
18. S. Kirkpatrick, C. D. Gelatt, Jr., and M. P. Vecchi, "Optimization by simulated annealing," *Science* **220**(4598), 671–680 (1983).
19. C. Y. Huang, C. H. Lin, Y. H. Chen, and Y. C. Huang, "Electro-optic Ti:PPLN waveguide as efficient optical wavelength filter and polarization mode converter," *Opt. Express* **15**(5), 2548–2554 (2007).

1. Introduction

Dual- or multi-line coherent light sources have attracted more and more attention because they are favorable to many applications such as remote sensing, optical communications, interferometry, biomedicine, and terahertz wave generation [1–3]. Such a source can be built in a laser system where a laser diode array or a solid-state laser with multiple gain lines has been used as the basis for the multiple wavelength selection and oscillation [4, 5]. However, the applicability of these laser systems can be quite restricted due to the limited spectral bands and range that can be offered by a laser. Optical parametric down conversion is a powerful technology that can extend the accessible spectral region from a single laser line (pump) to broad and continuous (single and idler) bands according to the energy conservation law, allowing reaching a desired application wavelength simply by varying the phase-matching condition of the conversion process. Moreover, rapid advances of the quasi-phase-matching (QPM) technology have contributed to the study of nonlinear optics besides the common application of the nonlinear gain enhancement. For example, the manipulation of the phase-matching spectrum of a nonlinear wavelength conversion process can be enabled through the highly engineerable characteristics of a QPM material based on, e.g., lithium niobate (LiNbO_3) crystals. For this aspect, optical parametric oscillators (OPO) oscillating at multiple signal/idler wavelengths have been demonstrated using a cascade-grating periodically poled lithium niobate (cg-PPLN) or an aperiodically poled lithium niobate (APPLN) providing multiple reciprocal vectors for phase-matching the multiple optical parametric down conversion processes [6, 7]. It has been shown that the aperiodic domain structuring technique exhibits many advantages over a cascade-grating structure in implementing multiple QPM channels in a nonlinear conversion process, including the high tailorability of the phase-matching spectrum and the full access of the device length for all the conversion channels [8, 9]. The tailorability facilitates the production of a specific multiline spectrum where the spectral heights and positions of the lines can be designed in great freedom, while a longer interaction length benefits the conversion process to acquire a higher nonlinear gain and a narrower output linewidth (and therefore leads to a higher spectral brightness).

A high brightness OPO is in demand for those applications aforementioned but usually realized in a pulsed pumping scheme (using usually a Q-switched laser). Pulsed pump lasers produce high peak power that benefits the down conversion efficiency due to the resultant high parametric gain. However, the signal/idler spectral bandwidth increases with increasing parametric gain, making against the building of a high resolution/precision/coherence system for most of the applications requesting a narrow-line source. Several methods have been used to reduce the output spectral linewidth of a (pulsed) OPO. Among these, the application of a wavelength selective element such as an etalon, a grazing-incident grating, a volume Bragg grating, or a birefringence filter in the oscillator has been a popular approach [10–12]. All

these elements work on specific wavelengths (spaced by the “free spectral range”) satisfying the relevant governing equations of the devices, limiting the applicability of being a multi-wavelength selector when free selection of the working spectral lines (e.g., multiple lines with nonuniform spacings) is desired. Besides, these elements work externally to the parametric gain medium, which is disadvantageous to the system integration and the total loss of the system. The passive operation of these elements also hinders them from being a versatile component in contrast to an active device (see below). The access to the electro-optic (EO) properties of a QPM material opens up new application frontiers for QPM technology. First, several interesting photonic devices including an EO polarization mode converter (PMC) [13] and an EO Bragg deflector [14] based on the spatial modulation of the EO coefficients (via the spatial modulation of the domain polarity) of QPM materials have been developed and successfully applied in laser and OPO systems [7, 15, 16]. Second, these active device functions can be readily built in a conventional QPM wavelength converter benefiting from the high domain-engineering ability of a QPM material, enabling the realization of highly integrated multi-function photonic devices with low insertion loss and high working efficiency. We have implemented a variety of such integrated QPM devices including a two-dimensionally domain structured LiNbO_3 crystal combining the functionalities of an EO Bragg deflector and an optical parametric down converter (OPDC) to achieve a pulsed multiline source [7]. Furthermore, a cascaded or an aperiodic domain structured LiNbO_3 device combining the functionalities of an EO PMC and an OPDC was realized to achieve a novel OPO source whose output spectrum can be narrowed and tailored via the fast EO control [15, 16]. However, the pulsed multiline source in [7] has a broad output spectral linewidth of ~ 0.8 nm (or ~ 100 GHz, which is almost unresolved by the International Telecommunication Union (ITU) grids), while the electro-optically spectrum narrowed OPOs in [15, 16] (and those OPOs using passive wavelength selective elements) work only on a single signal line (i.e., on one phase-matching channel).

In this work, we have designed and constructed an aperiodic domain structure in LiNbO_3 integrating the functionalities of a multi-channel EO PMC and a corresponding multi-channel OPDC in an all solid-state laser system to realize an EO controlled, highly narrowed multiline pulsed intracavity OPO (IOPO) source. This is, to the best of our knowledge, the first spectral narrowing mechanism working in a multiline OPO system with important advantages of allowing for a great freedom in the spectrum design and an integration with the OPDC thanks to the aperiodic optical superlattice (AOS) technique [17] employed in this work.

2. Core device design and simulation

The AOS technique has been a promising approach of constructing a domain structure providing multiple reciprocal vectors demanded in multiple QPM processes. In this study, a domain structure simultaneously satisfying the QPM conditions of an EO PMC and an OPDC working on the same (multiple) spectral lines has been derived using the AOS technique. To find an optimized domain structure (optimized with respect to the working efficiency of the two involved QPM devices, see below), an algorithm based on the simulated annealing (SA) method [18] has been developed, which is similar to a methodology reported in [16]. The built-in EO QPM PMC functions here as a multi-channel, narrowband notch-type spectral filter for narrowing the gain bandwidths of the down-converted signals at the corresponding channels. The working principle of an EO QPM PMC as a wavelength selective element in an OPO based on a QPM OPDC has been expounded elsewhere [15]. Mainly, an EO PMC (built in PPLN as an example) can perform energy conversion between the ordinary (o) and extraordinary (e) polarization modes of a wave in a narrow conversion bandwidth (~ 2 nm-cm at $1.5\text{-}\mu\text{m}$ band [19]) subject to the EO QPM condition. The conversion efficiency of the PMC is a function of the electric field (E_y) applied along the crystallographic y axis and can reach 100% at specific voltages at the phase-matching wavelength. The parametric gain bandwidth of a pulsed PPLN OPO (on the order of 1 nm [7, 16]) can be comparable to or

broader than the conversion bandwidth of a PPLN EO PMC (of a few centimeters long). Therefore, photons in a portion of the gain spectrum of the down-converted signal will be converted to the *o*-polarized wave, they will not be amplified effectively and will not reach the oscillation threshold if that spectral portion of the signal has been within the conversion bandwidth of the PPLN EO PMC working in the OPO cavity. This is because the type-0 (*eee*) QPM conversion process works only on the *e*-polarized wave. The output signal spectrum can thus be narrowed by this gain-spectrum suppression mechanism and can even be manipulated via the tuning of the applied electric field as the conversion (filtering) spectrum of the EO PMC is electric-field dependent [15, 16].

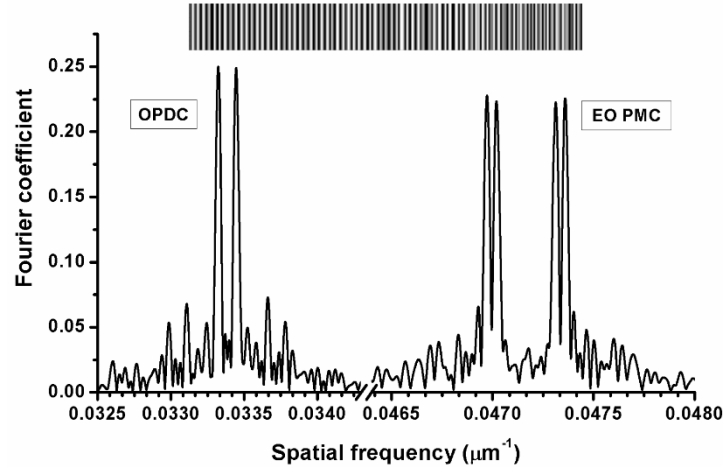


Fig. 1. Fourier spectrum of the calculated domain structure in LiNbO₃. Two and four target spatial frequencies, required for phase-matching the 1064-nm pumped 1540/3442 and 1550/3393 nm signal/idler OPG processes and for phase-matching the corresponding EO polarization-mode conversion processes at 40°C, respectively, are resolved. The inset schematically shows a section of the domain structure.

The developed SA algorithm mainly works on a calculation model built based on the coupled-wave theory describing the dual QPM devices (i.e., the multi-channel EO PMC and OPDC) to be integrated. The coupled-wave equations employed in our previous work [16] to calculate the behavior of single-channel devices are still valid for the present study. To yield a domain structure optimized for the requested multiple and multi-channel QPM processes, we applied an objective function (*OF*) to the algorithm to best achieve the target output performance of the involved QPM devices, given by

$$\begin{aligned}
 OF = & \left\{ \left(\sum_{\alpha=1}^M \left| \eta_{op,0}(\lambda_{s,\alpha}) - \eta_{op}(\lambda_{s,\alpha}) \right| w_{op}(\lambda_{s,\alpha}) \right) + \gamma_{op} (\max[\eta_{op}(\lambda_1), \dots, \eta_{op}(\lambda_M)] - \right. \\
 & \left. \min[\eta_{op}(\lambda_1), \dots, \eta_{op}(\lambda_M)]) \right\} + \left(\sum_{\beta=1}^N \left| \eta_{eo,0}(\lambda_{\beta}) - \eta_{eo}(\lambda_{\beta}) \right| w_{eo}(\lambda_{\beta}) \right) + \\
 & \left. \gamma_{eo} (\max[\eta_{eo}(\lambda_1), \dots, \eta_{eo}(\lambda_N)] - \min[\eta_{eo}(\lambda_1), \dots, \eta_{eo}(\lambda_N)]) \right\}, \quad (1)
 \end{aligned}$$

where M and N are the numbers of the conversion channels specified for the optical parametric down conversion and EO polarization-mode conversion processes, respectively, $\lambda_{s,\alpha}$ is the phase-matched signal wavelength associated to the α -th down-conversion channel, $\eta_{op,0}(\lambda_{s,\alpha})$ and $\eta_{op}(\lambda_{s,\alpha})$ (as defined in [16]) are the target and calculated conversion efficiencies of the OPO at $\lambda_{s,\alpha}$, $w_{op}(\lambda_{s,\alpha})$ is the weighting factor for the α -th down-conversion process, λ_{β} is the phase-matched wavelength associated to the β -th polarization-mode conversion channel, $\eta_{eo,0}(\lambda_{\beta})$ and $\eta_{eo}(\lambda_{\beta})$ (as defined in [16]) are the target and calculated efficiencies of EO PMC

at λ_β (located in the signal gain bandwidths), $w_{eo}(\lambda_\beta)$ is the weighting factor for the β -th polarization-mode conversion process, γ_{op} and γ_{eo} are adjustable parameters for equalizing the peak efficiencies of the multiple down-conversion and EO processes, respectively, and the operators $\max[\dots]$ and $\min[\dots]$ select the maximum and minimum values from the quantities enclosed in the square brackets. To build a high spectral brightness OPO, the signal gain bandwidth should be effectively reduced while the peak spectral gain can be best maintained. Such a goal has been pursued in the algorithm. The calculated domain structure exhibits a barcode-like pattern, as schematically shown in the inset of Fig. 1 (only a section of the structure is shown). The black and white stripes denote the opposite domain polarities. The total length of the structure is 3 cm. The thickness of the unit domain block [17] for constituting the structure is 4 μm . Figure 1 shows the Fourier spectrum of the calculated domain structure in LiNbO₃ (which is an aperiodically poled lithium niobate (APPLN)). Two target spatial frequencies at 0.03344 and 0.03332 μm^{-1} , required for quasi-phase-matching the 1064-nm pumped 1540/3442 and 1550/3393 nm signal/idler optical parametric generation (OPG) processes at 40°C, are resolved from the Fourier analysis, while another group of frequencies at 0.04736, 0.04731, 0.04702, and 0.04697 μm^{-1} is also resolved as expected for phase-matching the corresponding EO polarization-mode conversion processes (at wavelengths 1539.39, 1540.66, 1549.38, and 1550.62 nm at 40°C) for achieving the desired gain spectrum tailoring. The OF parameters $M = 2$, $N = 4$, $\lambda_{s,\alpha} = 1540$ and 1550 nm with $w_{op}(\lambda_{s,\alpha}) = 16$ for $\alpha = 1$ and 2, respectively, $\gamma_{op} = 3$, $\lambda_\beta = 1539.39$, 1540.66, 1549.38, and 1550.62 nm with $w_{eo}(\lambda_\beta) = 2$ for $\beta = 1, 2, 3$, and 4, respectively, and $\gamma_{eo} = 2$ were used in the calculation.

Figure 2(a) shows the calculated single-pass *e*-wave transmission spectrum at $E_y = 150$ V/mm and OPO signal spectrum based on 7 cavity roundtrips for signal buildup at $E_y = 0$ V/mm when an *e*-polarized wave with a flat spectrum over 1520-1560 nm (calculation range) and a 6 MW/cm² *e*-polarized wave at 1064 nm are incident at the domain structure, respectively. All the calculations on the outputs of the APPLN device and the IOPO in this study were carried out with a calculation model based on the coupled-wave theory [16]. The number of the cavity roundtrips and the pump level assumed in the calculation is to produce signals of linewidth around ~ 1 nm based on the IOPO configuration built in this work (see section 3). As shown in Fig. 2(a), the *e*-wave transmission spectrum of the domain structure (i.e., the APPLN) under $E_y = 150$ V/mm has two spectral peaks located around the peak wavelengths of the two OPO signals with their spectral linewidths (~ 0.6 nm) narrower than those OPO signals (0.8-0.9 nm), achieving the goal of spectral narrowing by suppressing the lower gain portions while maintaining the peak gain regions of the signal oscillation bands. Multiline signal with drastically increased power spectral density can thus be expected from such a gain spectrum tailoring technique where only the high spectral gain regions of the signals are nonlinearly (exponentially) amplified. Figure 2(b) shows the calculated output signal spectrum (blue line) from an IOPO constructed using the APPLN device (refer to section 3 for the system configuration used in an experimental demonstration) at $E_y = 150$ V/mm under intracavity 1064-nm pump intensity of 6 MW/cm² and 7 cavity roundtrips for signal buildup. The result shows the spectral peak heights and widths of the signals have been increased and reduced by ~ 3.5 and ~ 80 times, respectively, in contrast to those (red line) from the system operated in the passive mode (i.e., at $E_y = 0$ V/mm), leading to a great enhancement of the signal power spectral density.

It is interesting to investigate the temperature effect on the output spectrum of the electro-optically controlled, dual-wavelength APPLN IOPO. The APPLN device integrates the functionalities of an OPDC and an EO PMC whose output spectra are tunable with temperature but with dissimilar tuning characteristics described by their respective QPM conditions (e.g., the tuning rates are 0.27 and -0.66 nm/°C for the OPDC and EO PMC, respectively, at the 1550 nm band). It is thus possible to use the present technology to perform the spectral tuning/tailoring of the signal with temperature as long as the (dual) pass bands of

the EO PMC are within the corresponding parametric gain bandwidths according to the gain-spectrum suppression mechanism as illustrated in Fig. 2(a). Figures 2(c) and 2(d) show the simulated output spectra of the IOPO under the EO control (at $E_y = 150$ V/mm) at the 1540 and 1550 nm signal bands, respectively, for several different operating temperatures. The results suggest that the signal spectrum can be well retained within the 0.1 °C temperature fluctuation. Besides, the results obtained at an operating temperature of 40.5 °C show it is possible to tune the dual-wavelength signal of the IOPO with temperature (a red shift of 0.013 and 0.012 nm for the 1540 and 1550 nm spectral peaks, respectively), manifesting an important advantage of this unique technology.

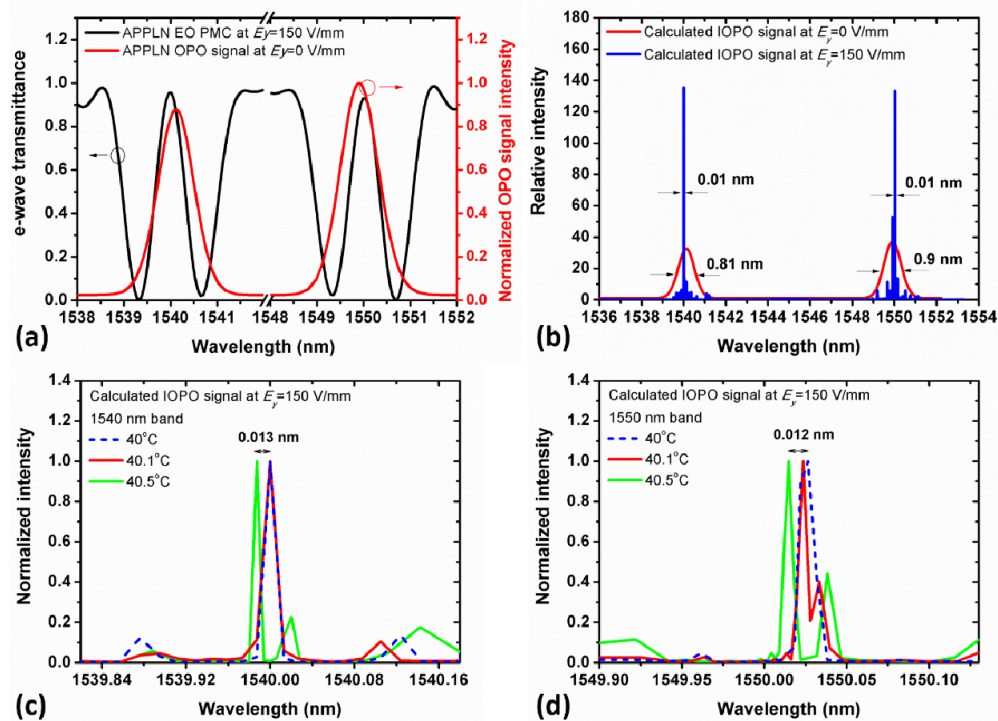


Fig. 2. (a) Calculated single-pass *e*-wave transmission spectrum at $E_y = 150$ V/mm and OPO signal spectrum based on 7 cavity roundtrips for signal buildup at $E_y = 0$ V/mm when an *e*-polarized wave with a flat spectrum over 1520-1560 nm and a 6 MW/cm² *e*-polarized wave at 1064 nm are incident at the APPLN, respectively. (b) Calculated output signal spectra from an IOPO constructed using the APPLN device at $E_y = 0$ V/mm (red line) and 150 V/mm (blue line) at 40°C. (c) and (d) Simulated output spectra of the IOPO under the EO control (at $E_y = 150$ V/mm) at the 1540 and 1550 nm signal bands, respectively, for several different operating temperatures.

The present technology can be readily applied to implement an IOPO system for a higher number of spectral lines (though demanding a more involved calculation process). As an example, Fig. 3(a) shows the Fourier analysis of an APPLN calculated for a three spectral-peak (1530, 1540, and 1550 nm) system by following the methodology presented above, while Fig. 3(b) shows the calculated IOPO signal spectrum based on the APPLN at $E_y = 200$ V/mm under intracavity 1064-nm pump intensity of 6 MW/cm² and 11 cavity roundtrips for signal buildup.

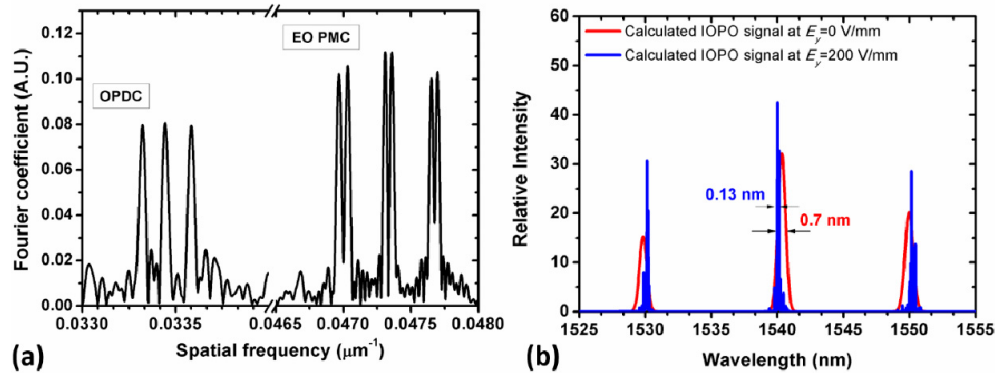


Fig. 3. (a) Fourier analysis of an APPLN calculated for a three spectral-peak (1530, 1540, and 1550 nm) system. (b) Calculated IOPO signal spectrum based on the APPLN at $E_y = 200$ V/mm under intracavity 1064-nm pump intensity of 6 MW/cm^2 and 11 cavity roundtrips for signal buildup.

3. Device fabrication, IOPO construction, and output performance characterization

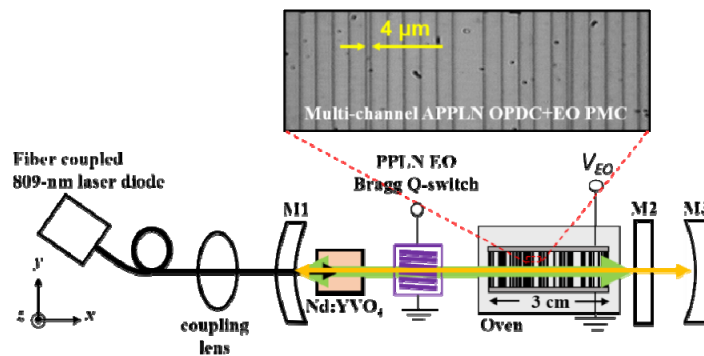


Fig. 4. Schematic arrangement of an EO spectral-line controlled/narrowed, multiline OPO achieved using the constructed APPLN device in a diode-pumped, EO Q-switched Nd:YVO₄ laser. The inset shows an image of a portion of the HF-etched + z surface of the APPLN crystal.

To conduct a proof-of-principle demonstration of the proposed multiline gain spectrum tailoring technique, we fabricated the APPLN device as designed in section 2 for the application to a dual-wavelength IOPO. The binary (± 1) content of the APPLN domain structure, composed of 7500 unit domain blocks with each having a thickness of $4 \mu\text{m}$, is translated into a photomask for the subsequent lithographic and electric-field poling process made in a 30-mm-long, 1-mm-wide, and 0.5-mm-thick z -cut LiNbO₃ chip. Both end (x) faces of the fabricated APPLN crystal were anti-reflection coated for wavelengths at 1064 and 1500-1580 nm, while the two y faces of the crystal were sputtered with NiCr alloy as the electrodes for the E_y application. Figure 4 shows the schematic arrangement of an EO spectral-line controlled/narrowed, multiline OPO achieved using the constructed APPLN device in a diode-pumped, EO Q-switched Nd:YVO₄ laser. The inset shows an image of a portion of the HF-etched + z surface of the APPLN crystal, indicating the constituent domains have thicknesses a multiple of $4 \mu\text{m}$. The APPLN device was installed in a crystal oven maintaining a constant temperature of 40°C (stabilized within $\pm 0.1^\circ\text{C}$). The laser gain medium is an a-cut 0.3-at. % Nd:YVO₄ crystal, having a 9 mm length and a $3 \text{ mm} \times 3 \text{ mm}$ clear aperture. The pump laser is a fiber coupled diode laser centered at 809 nm. A 15-cm

radius-of-curvature (ROC) meniscus dielectric mirror (M1) and a plane-plane dielectric mirror (M2) form a laser resonator for oscillating the 1064-nm wave. Mirror M1 has ~93% transmittance at 809 nm and ~99.8% and >99.4% reflectance at 1064 and 1510-1560 nm, respectively, while mirror M2 has ~99.6% reflectance at 1064 nm and >99.3% transmittance at 1510-1560 nm. The 1064-nm laser is Q-switched by a homemade PPLN EO Bragg cell [14]. An efficient Q-switching in such a high finesse laser cavity can only be accomplished via the effective laser energy dumping through the optical parametric down-conversion in the APPLN device. The down-converted multiline signals build up in an IOPO formed by mirror M1 and an output coupler (M3). M3 is a ROC = 15 cm, plano-concave dielectric (BK7) mirror having ~97% reflectance at 1510-1560 nm.

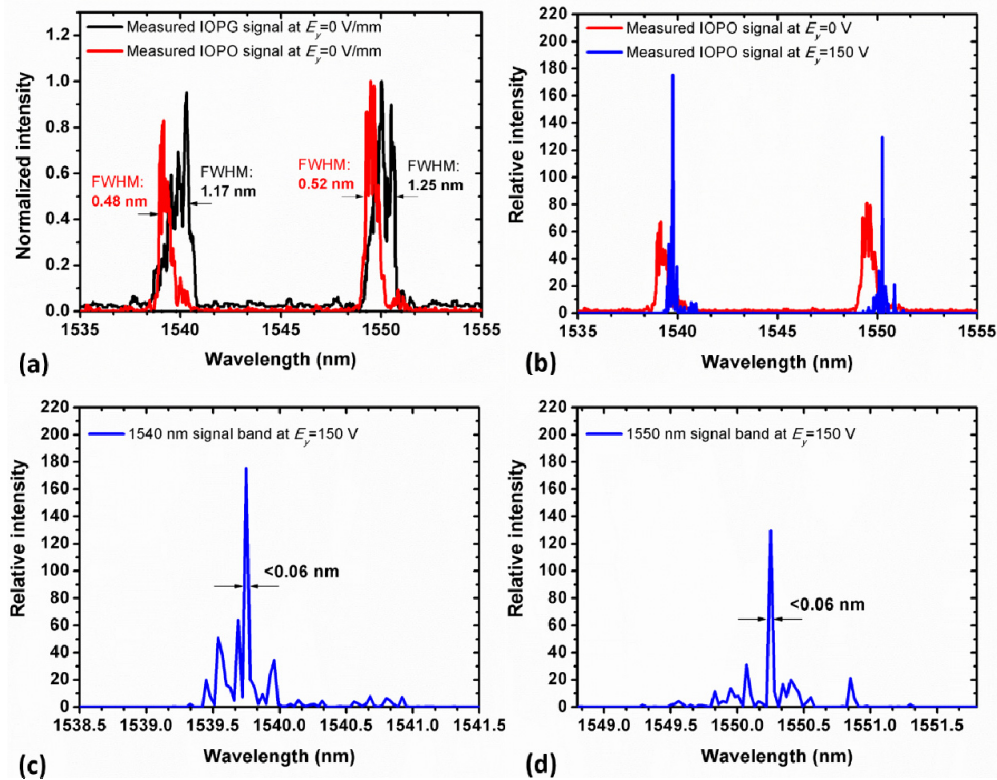


Fig. 5. (a) Measured normalized IOPG (black line) and IOPO (red line) signal spectra when the system shown in Fig. 4 was pumped at ~5 W diode power. (b) Measured signal spectra of the IOPO when the APPLN device is applied with $E_y = 0$ V/mm (red line) and 150 V/mm (blue line). (c) and (d) Expansion of signal spectrum from Fig. 5(b) at the 1540 and 1550 nm bands for the IOPO under EO control, respectively.

We first worked the system as a pulsed IOPO in the passive mode (i.e., with $E_y = 0$ V/mm) by driving the PPLN EO Bragg cell with a 170-V, 300-ns voltage pulse train at 1 kHz but without the application of any voltage to the APPLN device. Figure 5(a) shows the measured normalized OPO signal spectrum (red line) when the system was pumped at ~5 W diode power. The spectral linewidths of the dual-wavelength signal at $E_y = 0$ V/mm are about 0.5 nm, a bit narrower than those design values (red-line signal in Fig. 2(b)) mainly due to the acquisition of a smaller nonlinear gain than expected (which could arise from the non-ideal domain poling quality) and the limit of the available diode pump power. Yet this discrepancy verifies a high design tolerance with the present technology according to the experimental results shown below. The normalized single-pass OPG signal spectrum (black line in Fig.

5(a)) was also measured (by removing the mirror M3) for the comparison. It was found that the OPG signals emerge at 1540 and 1550 nm and exhibit almost the same spectral height, which is in line with the goal set in the design algorithm. The OPO signals, however, slightly deviated from the designed spectral positions (blue-shifted from 1540 and 1550 nm by ~ 0.85 and ~ 0.5 nm, respectively). The deviation can be attributable to the present algorithm, which assumes a uniform cavity condition such as uniform cavity losses for all the (signal) spectral elements of interest in the core (APPLN) device design and simulation. The OPO signal spectrum in Fig. 5(a) thus presents a result of the gain competition of modes (in the gain bandwidth) on the basis of the non-uniform (spectral dependent) cavity condition associated to the built system. When the IOPO is operated in the active mode (i.e., when an electric field E_y is applied to APPLN device), the output signal spectral shape can be varied (including a narrowed spectrum as desired) with the change of E_y due to the unique EO gain spectrum tailoring mechanism discussed above. Figure 5(b) shows the measured signal spectrum (blue line) of the IOPO when $E_y = 150$ V/mm is applied to the APPLN device. The diode pump power was again at ~ 5 W. No obvious variation in the output signal spectrum is found from measurement to measurement. The output result for the IOPO operated in the passive mode is also plotted (red line) here for the comparison. Figures 5(c) and 5(d) show the expansion of signal spectrum from Fig. 5(b) at the 1540 and 1550 nm bands for the IOPO under the EO control, respectively. The values of the spectral linewidths of the dual signals from the IOPO under the EO control have both reached the resolution limit (0.06 nm) of the employed optical spectrum analyzer (Agilent 86142B), though even narrowed linewidths of 0.01 nm have been predicted (see Fig. 2(b)). Thus the measured spectral linewidths have been remarkably narrowed by a factor of >8 and >8.7 , while the peak spectral intensities have been enhanced by ~ 2.5 and ~ 1.6 times, for the 1540 and 1550 nm signals, respectively, when compared to the output of the system in passive mode. From Fig. 5(c), we found the intensity ratio between the main spectral peak and side bands is about 3, leading to a lowered contrast of the main spectral peak which is 92% (with respect to the local minimum. The contrast can be as high as 99.2% for the main spectral peak at the 1550 nm band though) due to an elevated background intensity level caused by the nearby side bands. Signal side bands can be possibly suppressed by creating broader notch dips in the transmission spectrum of the APPLN under the EO control (refer to Fig. 2(a)) to increase the free spectral range and to further narrow the pass bands for tailoring a more satisfactory signal spectrum. This can be done by applying more but appropriately allocated phase-matching channels in the EO PMC calculation (i.e., by setting λ_β for a larger N in Eq. (1)), which, however, entails a complicated and time-consuming computation work. The measured highly-narrowed dual-wavelength signal spectrum under the EO control was in reasonable agreement with that simulated in Fig. 2(b); the discrepancy between the measured and predicted results can originate from the blue-shifted signals observed in the passive mode as discussed above. Consider the measured output signal energies of 0.631 and 0.512 μJ (corresponding to peak powers of 140 and 114 W) from the IOPO operated in the passive ($E_y = 0$ V/mm) and active ($E_y = 150$ V/mm) modes, respectively, we estimated an enhancement of the power spectral density of the EO controlled system to be a factor of ~ 7.8 . Figure 6 shows the measured temporal behavior of the system output, exhibiting signal pulses having a pulse width of ~ 4.5 ns and a peak-to-peak intensity fluctuation of $\sim 7\%$.

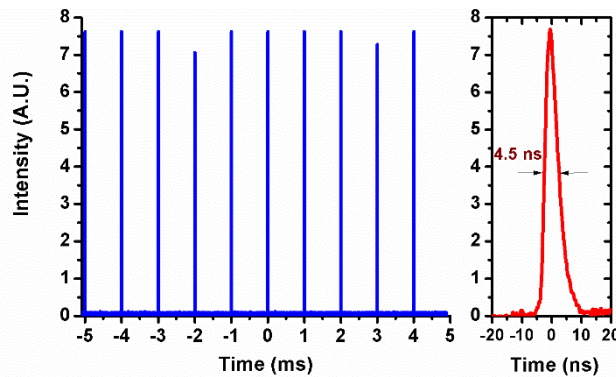


Fig. 6. Measured temporal behavior of the IOPO output. Left: peak-to-peak intensity fluctuation. Right: a typical signal pulse shape.

4. Conclusion

We have developed a design methodology based on the AOS technique to construct a novel APPLN for integrating the functionalities of a multi-channel EO PMC and a corresponding multi-channel OPDC in a 1064-nm Nd:YVO₄ laser system to realize an EO controlled, highly narrowed multiline pulsed IOPO source at 1.5 μm bands. When the IOPO is operated in the active mode (i.e., when an electric field E_y is applied to APPLN device), the output signal spectral shape can be varied with the change of E_y via the unique EO gain spectrum tailoring mechanism. In this way, we obtained from the APPLN IOPO under the EO control (at $E_y = 150$ V/mm) the output of a dual-wavelength signal at 1540 and 1550 nm whose spectral linewidths have been remarkably narrowed by a factor of >8 and >8.7 , while the peak spectral intensities have been enhanced by ~ 2.5 and ~ 1.6 times, respectively, when compared to the output of the system in passive mode, indicating a largely increased power spectral density of the source.

Funding

Ministry of Science and Technology of Taiwan (MOST) (105-2221-E-008-066, 104-2923-E-007-001-MY4).

Acknowledgments

The authors thank the Thin Film Technology Center (TFTC) at National Central University, Taiwan, for offering the service of the optical coatings.